



The salinity anomalies due to the biogeochemical processes in the Bohai Sea

Fengying Ji¹, Xunjun Xiong²

¹National Marine data and information service, Tianjin, 300171, China

5 ²Ocean College, Zhejiang University, Zhoushan City, Zhejiang Province, 316021, China.

Correspondence to: Fengying Ji (2320130582@qq.com)

Abstract. Salinity has been classed as an 'Essential Climate Variable' by the Global Observing System for Climate since 2010 and its compatibility must be ensured to avoid spurious trends and discontinuities. Because of the lack of measurements, it is not well known that small variations in the relative dissolved constituents of coastal and semi-enclosed seawater result in changes in the Absolute Salinity S_A which is the salinity parameter of the International Thermodynamic Equation of Seawater – 2010 (TEOS-10 for short), and the changes in the Practical Salinity S_p that it results in, which is still served as the simplicity of Absolute Salinity in many studies, are even less well known. To clarify the salinities compatibility level in the semi-enclosed Bohai Sea, we analyzed the repeat in-situ measurements along the section from 1985 to 2020 and the near-synchronous field data from 2006 to 2007 in this sea, found the main relative composition anomalies are dominated by additional HCO_3^- and Ca^{2+} which mainly originate from the suspension and redissolution of bottom sediments. They can increase the S_A by a maximum of $0.1 \text{ g}\cdot\text{kg}^{-1}$ and raise the S_p of $0\sim 0.04 \text{ PSS-78}$ according to the TEOS-10 algorithm and the mathematical model Pa08. Moreover, we parameterized the δS_A and δS_p with their uncertainties with/without considering relative composition variations in the Bohai Sea respectively. All the results may provide a reference for salinity research in semi-closed oceans.

1 Introduction

20 Salinity is a parameter used to quantify the total mass of inorganic substances dissolved in seawater and has been classed as an 'Essential Climate Variable' (GCOS, 2010) for observing, modelling, and analysing the increasing effects of global warming on ecosystems and society. Consistency and compatibility of salinity must be ensured to avoid spurious trends and discontinuities (Feistel et al., 2016), hence the uncertainty level of $0.002 \text{ g}\cdot\text{kg}^{-1}$ in the dissolved mass fraction required for routine research and monitoring (Seitz et al., 2011).

25 Due to the complexity of dissolved components in seawater, until now, routine salinity measurements have so far been acquired by specific measurement techniques applied to a proxy property of seawater, such as chlorinity and electrical conductivity based on the assumption that the relative composition of dissolved matter remains constant. However, the effect of slight variations in the relative chemical composition of seawater on salinity, as shown in global scale observations, has been taken into account by the new seawater standard TEOS-10 (IOC et al., 2010) and provide a correction factor (so-called 'Absolute



30 Salinity Anomalies', denoted by δS_A) which characterizes the effect of these relative compositional changes on seawater density is used to determine the Absolute Salinity (S_A). Available studies found that δS_A ranged from 0 to $0.030 \text{ g}\cdot\text{kg}^{-1}$ with an uncertainty of $\pm 0.01 \text{ g}\cdot\text{kg}^{-1}$ in the open ocean (McDougall et al, 2012), $0.087 \pm 0.028 \text{ g}\cdot\text{kg}^{-1}$ in the Baltic Sea (Feistel et al, 2010), spanned 3 orders of magnitude from 0.005 to $0.6 \text{ g}\cdot\text{kg}^{-1}$ in river mouths (Pawlawz, 2015), varied from -0.05 to $0.28 \text{ g}\cdot\text{kg}^{-1}$ of China off-shore waters from 2006 to 2007 (Ji et al, 2021).

35 In some studies, there is a need to maximize the simplicity of the procedure while accepting a reduction in accuracy, such as in the detection of salinity changes associated with climate change, where precision may be more important than accuracy, and therefore the Practical Salinity S_P is still used as the as a proxy of Absolute Salinity S_A and the relative compositions anomalies is ignored (WOA18: Zweng et al, 2019; Chen,1992). Although non-ionized silicates dominate the composition anomaly in the open ocean which has a very small effect on the S_P , the relative composition anomaly of the North Pacific Intermediate Water
40 (NPIW) which is normalized to have the same chlorinity as SSW76 results in the Practical Salinity change δS_P about 0.0062 PSS-78 according to the quantitative studies of Pawlowicz (2008, 2009, 2010).

However, δS_A and δS_P are still not well understood for estuaries and semi-enclosed oceanic basins where the relative composition anomalies of the seawater may be somewhat different from that of the open ocean and may change over relatively short periods. The available relevant studies show that mean calcium concentrations increased significantly by about 4%
45 between 1966/69 and 1994/95(Feistel et al., 2010). The δS_A near the mouth of the Yellow River in the Bohai Sea is not only twice as high as that calculated by the Pawlowicz model but the data of δS_A are scattered and messy (Ji et al., 2021) indicating its variation characterization is not accurately captured.

The Bohai Sea is not only a typical semi-closed ocean but also has accumulated oceanography measurements with a period of 1957-2020 and a spatial resolution of up to 10km, which allows us to obtain its biogeochemical processes at different spatial
50 and temporal scales, to accurately characterize the salinity anomalies induced by specific biogeochemical processes, which have been overlooked in studies of salinity variations associated with climate change (Lin et al, 2001; Ma et al, 2006; Xu, 2007; Lv, 2008; Song, 2009; Yu et al, 2009).

The purpose of this paper is to accurately characterize the δS_A and δS_P based on a long time series of measurements and to specify the compatibility level of long-term salinity change of the Bohai Sea with/without consideration of relative composition
55 variations. The algorithm of δS_A and δS_P and the data used in this study are provided in Sect. 2. The magnitude, distribution characteristics, and decadal change patterns of the relative composition anomalies, δS_A , and δS_P , as well as the parameterization formulas for calculating δS_A , and δS_P are given in Sect.3. At last, a summary of the results of the study, its limitations, and the ongoing continuation of the work are given in Sect. 4.



2 Methods and data

60 2.1 Methods for estimating the Absolute Salinity Anomaly δS_A in TEOS-10

The new equations of state TEOS-10 introduce different Absolute Salinity Variables to represent the different influences of dissolved material on the thermodynamic properties of seawater because no single salinity variable can fully represent the influence when composition anomalies are present in seawater. One of the most used of these variables is “Density Salinity”, represented by the symbol S_A^{Dens} , which is designed to accurately calculate the density ρ of a seawater sample with salinity

65 S_A^{Dens} ,

$$\rho = f_{\text{TEOS-10}}(S_A^{\text{Dens}}, t, p) \quad (1)$$

where $f_{\text{TEOS-10}}$ is a precisely specified function derived from the TEOS-10 Gibbs function of seawater, t is the temperature, and p is the pressure (Feistel, 2008). The primary purpose of oceanographic salinity measurements is to calculate the density of seawater to estimate currents that are driven by horizontal pressure gradients. Concerning TEOS-10, the Absolute Salinity

70 in this paper refers specifically to the Density Salinity, so S_A^{Dens} is simplified as S_A .

Since both roles of salinity, as a density state variable and as a measure of dissolved material, are important, another popular Absolute Salinity variable of the TEOS-10 is Solution Absolute Salinity S_A^{soln} which is based on adding up the mass of solute in a seawater sample,

$$S_A^{\text{soln}} = \sum_{i=1}^{N_c} M_i c_i \quad (2)$$

75 Where c_i is the molar concentration of component i in seawater per kilogram, M_i is the molar mass of the component, and N_c is the number of species of the component in seawater.

It should be noted that, for real seawaters with a slightly different composition, Eqs. (1) and (2) do not result in the same values (Pawlowicz et al., 2011) due to changes in the halide concentration coefficient, implying that $S_A \neq S_A^{\text{soln}}$ in general. In this case, the formula for conversion between to S_A^{soln} and S_A^{soln} is provided in TEOS-10.

80 The first approximation for S_A is provided by the Reference Salinity S_R ,

$$S_R = (35.16504/35) \cdot S_p, \quad 2 < S_p < 42 \quad (3)$$

(Millero et al., 2008a) which neglects the generally small composition anomalies in seawater and first defines a stoichiometric composition model (the Reference Composition or RC), therefore providing results essentially equivalent to past practice with the commonly used Practical Salinity S_p .

85 In most cases, ordinary seawater can be regarded as standard seawater concentrated/diluted with pure water and mixed with small amounts of other ingredients. If Absolute Salinity S_A is calculated from the Reference Salinity S_R , the Absolute Salinity Anomaly δS_A needs to be added,

$$S_A = S_R + \delta S_A \quad (4)$$



At present three practical algorithms to calculate the δS_A in the open ocean are provided by TEOS-10. First, assuming that the
 90 added components are not only in small amounts but also that the molar volumes are similar to the values of the main
 components of SSW, the haline contraction coefficient of seawater is 0.7519, which is the same as that of SSW.

First, on the assumption that the added components are not only in small amounts but also that the molar volumes are similar
 to the values of the main components of SSW, the haline contraction coefficient of seawater is 0.7519, which is the same as
 that of SSW.

95 The δS_A is determined by the density difference between the sample with the SSW in the laboratory $\delta\rho/(\text{kg} \cdot \text{m}^{-3}) = \rho^{lab} - \rho(S_R, 25^\circ\text{C}, 0 \text{ dbar})$ (McDougall et al., 2012; Millero et al., 2008a),

$$\delta S_A/(\text{g} \cdot \text{kg}^{-1}) = \delta\rho * 0.7519 \text{ g} \cdot \text{kg}^{-1}/(\text{kg} \cdot \text{m}^{-3}) \quad (5)$$

Second, δS_A can be regressed onto the concentrations of $S_i(\text{OH})_4$ based on the practical salinity, density, and silicate
 concentration data of 811 seawater samples worldwide (McDougall et al., 2012),

100
$$\delta S_A/(\text{g} \cdot \text{kg}^{-1}) = R^\delta S_R \quad (\text{except the Baltic Sea}) \quad (6)$$

in which, $R^\delta = \delta S_A^{\text{atlas}}/S_R^{\text{atlas}}$, both the S_R^{atlas} and $\delta S_A^{\text{atlas}}$ are from the McDougall et al (2011) hydrographic atlas.

Third, δS_A can be estimated by a correlation equation when the most variable seawater constituents, i.e., the carbonate system
 and macro-nutrients in the open ocean are also available,

$$\delta S_A^{\text{dens}}/(\text{mg} \cdot \text{kg}^{-1}) = 55.6 \times \Delta[\text{NTA}] + 4.7 \times \Delta[\text{NDIC}] + 38.9 \times [\text{NO}_3^-] + 50.7 \times [S_i(\text{OH})_4] \quad (7)$$

105 The units of each component on the right are all $\text{mmol} \cdot \text{kg}^{-1}$, $\Delta[\text{NTA}] = \text{TA} - 2.3 \times \frac{S_P}{35}$ is the standardized change in Total
 Alkalinity ΔTA , and $\Delta[\text{NDIC}] = \text{DIC} - 2.08 \times \frac{S_P}{35}$ is the standardized change in Total Dissolved Inorganic Carbon, ΔDIC .

Note that the coefficients of this model are calculated using a numerical model for chemical interactions (Pawlowicz et al.,
 2008, 2010, 2011; IOC et al., 2010), which performed well against lab studies, and were shown to have reasonable accuracy
 for seawater samples by Ryan (2014). An important aspect of this modeling is to maintain a charge balance in the dissolved

110 constituents, it was assumed that calcium concentrations also changed according to the:

$$\Delta[\text{NTA}] = 2\Delta\text{N}[\text{Ca}^{2+}] - \Delta[\text{NO}_3^-] \quad (8)$$

Calcium was chosen to balance the charge because a) it is not usually measured, but b) it is known to vary in relative
 composition by a few percent in the open ocean. Nevertheless, the accuracy of this relationship is uncertain (Pawlowicz, 2010).

2.2 Mathematical model Pa08 to calculate the δS_p resulting from the composition perturbation

115 The mathematical model κ_{Pa08} is used to test the electrical conductivity of an aqueous solution by summing all the ionic
 equivalent conductivities associated with all the ions in the solution. The simplified equation is as follows (Pawlowicz, 2008,
 2010):

$$\kappa_{Pa08}(C) = \sum_{i=1}^{N_c} \bar{\lambda}_i c_i^* z_i \quad (9)$$

Where C is the composition of ions in solution, N_c is the number of species of ions in solution, $\bar{\lambda}_i$, c_i^* , and z_i are the



120 equivalent conductivity per mole, valence, and the corresponding chemical equivalent ion concentration of the i^{th} ion.
 There may be a difference between the conductivity $\kappa_{Pa08}(C)$ and the true conductivity $\kappa(C)$ since these ionic equivalent
 conductivities are susceptible to screening effects from nearby ions, which increase with the ionic strength of the solution
 and are also affected by specific interionic pairing interactions. Assuming the discrepancy $\varepsilon \approx \text{const}$, based on the chemical
 composition of the Standard Sea Water (SSW for short), the Pa08 model parameterizes the ε by

$$125 \quad \kappa(C_*) = \kappa_{Pa08}(C_*) \cdot (1 + \varepsilon)^{-1} \quad (10)$$

In which, C_* is the chemical composition of the SSW and $\kappa(C_*) = f_{78}^{-1}(S_{p*})$. When there is a perturbation δC_* in the
 composition of SSW, the conductivity is calculated by

$$\kappa(C_* + \delta C_*) = \kappa_{Pa08}(C_* + \delta C_*) \cdot (1 + \varepsilon)^{-1} \quad (11)$$

For non-standard seawater with a measured S_p whose actual composition is $\beta C_R + \delta C_*$, in which C_R is the composition of
 130 the SSW, β is the dilution factor for the SSW. When the perturbation δC_* is known, β can be found by iteratively solving

$$\kappa(\beta C_R + \delta C_*) = \kappa(C_R) \quad (12)$$

Then the Practical Salinity Anomaly δS_p caused by the perturbation δC_* is calculated by

$$\begin{aligned} \delta S_p &= S_p(\beta C_R + \delta C_*) - S_p(\beta C_R) \\ &= f_{78}(\kappa(\beta C_R + \delta C_*)) - f_{78}(\kappa(\beta C_R)) \\ &\approx f_{78}(\kappa(\beta C_R) + \delta \kappa_{Pa08}(1 + \varepsilon)^{-1}) - f_{78}(\kappa(\beta C_R)) \end{aligned} \quad (13)$$

135

2.3 Oceanographic and ocean chemical data in the Bohai Sea

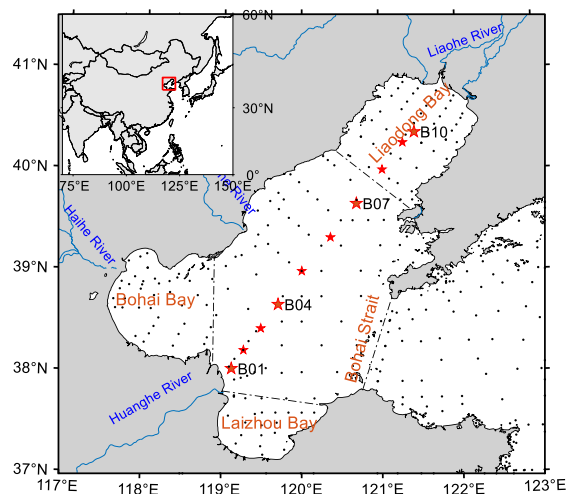
Section B runs through the Bohai Sea in the southwest-northeast direction, with the estuary of the Yellow River, China's
 second-largest runoff, at the southwest end, the mouth of the Liaohe River at the northeast end, and four stations in the middle
 directly facing the Bohai Strait which is only water exchange channel of the Bohai Sea. Therefore, Section B essentially
 140 characterizes the Bohai Sea as it reflects the impact of land-sourced runoff on the Bohai Sea, as well as the impact of the
 exchange between the Bohai Sea and the open ocean.

There are 10 stations in Section B, as shown in Fig.1. Repeat hydrographic measurements accompanied by synchronized
 seawater sampling to obtain nutrients, TA, and pH, are conducted annually in February and August. 2993 ocean water samples
 from 1985 to 2020 are used in this study.

145 The data analyzed in this study were collected from 290 stations established by the Marine Integrated Investigation and
 Evaluation Project of the China Sea (MIIEP), which was conducted by the State Oceanic Administration of China (Xiong,
 2012; Ji, 2016). These stations are depicted in Fig.1. Nutrient, TA, and pH measurements were obtained at four different depths
 (surface, 10 m, 30 m, and bottom) of these stations during the summer (August) of 2006 and winter (January) of 2007.



150 Since there is no in situ measurement of DIC in Section B and MIIEP, $\Delta[\text{NDIC}]$, $\Delta[\text{CO}_3^{2-}]$, and $\Delta[\text{HCO}_3^-]$ are calculated from pH and TA measurements using the CO2SYS software, which was released by the Department of Ecology of Washington State, USA which is based on the carbonate equilibrium (Lewis and Wallace, 2021). Additionally, $\Delta[\text{Ca}^{2+}]$ is derived from the ΔNTA and $[\text{NO}_3^-]$ based on Eq. (8).



155 **Figure 1.** The geographical distribution map of sampling stations, in which the red pentagrams '★' are the sampling stations of Section B, and the black dots '•' are the sampling stations of the MIIEP of the China Sea.

3 Result

3.1 Nutrients and inorganic carbon in the Bohai Sea

160 As shown in Figs. 2 and 3, the relative composition anomalous of the Bohai Sea water is dominated by the $\Delta[\text{HCO}_3^-]$ and $[\text{Ca}^{2+}]$, whose concentrations are more than $0.3\text{mmol}\cdot\text{kg}^{-1}$, while the concentrations of other nutrients are at least one order of magnitude lower than this value. $[\text{Si}(\text{OH})_4]$, as the primary relative composition anomaly in the open ocean, is present here at a concentration of less than $0.02\text{mmol}\cdot\text{kg}^{-1}$, and the same goes for $[\text{NO}_3^-]$, the concentration of phosphate is less than $0.001\text{mmol}\cdot\text{kg}^{-1}$ and is ignored in this study.

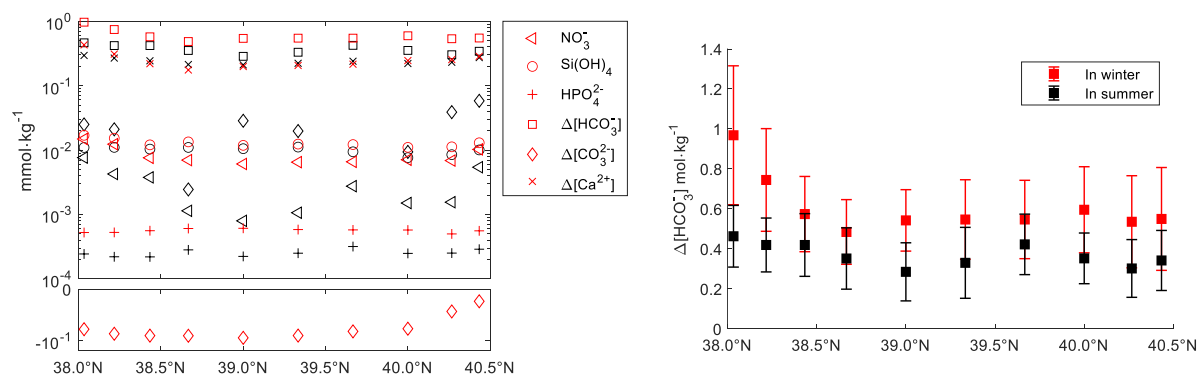


Figure 2. The left is the multi-year mean $[\text{NO}_3^-]$, $[\text{Si}(\text{OH})_4]$, $[\text{HPO}_4^{2-}]$, $\Delta[\text{HCO}_3^-]$, $\Delta[\text{CO}_3^{2-}]$ and $\Delta[\text{Ca}^{2+}]$ of 10 stations of section B in summer (in black) and winter (in red) from 1985 to 2020, the right is the multi-year mean of $\Delta[\text{HCO}_3^-]$ with a corresponding standard deviation of Section B.

165

The minimum of nutrients and dissolved inorganic carbon occurs in the middle of the Bohai Sea Strait as the hub of internal and external water exchange of the Bohai Sea and increases gradually in the west, south, and north directions. The maximum is in Bohai and Liaodong Bays on both sides of the Yellow River estuary. Except for $\Delta[\text{CO}_3^{2-}]$, they are much higher in winter than in summer, and slightly higher at the bottom than at the surface. The only one of these dissolved components that is less than 0 is $\Delta[\text{CO}_3^{2-}]$ in winter, which ranges from $-0.1 \text{ mmol} \cdot \text{kg}^{-1}$ to 0, because a portion of $[\text{CO}_3^{2-}]$ ions react with CO_2 and form $[\text{HCO}_3^-]$ ions according to the thermodynamic equilibrium conditions of the marine CO_2 system of the Bohai Sea.

170

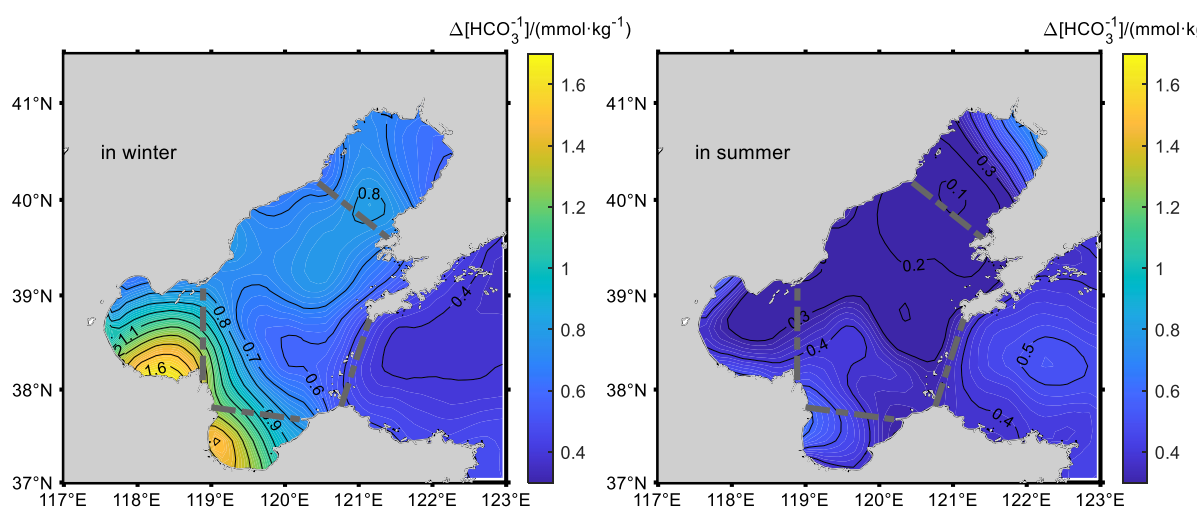


Figure 3. The $\Delta[\text{HCO}_3^-]$ of MIEP in the bottom of the Bohai Sea during the summers of 2006 and the winter of 2007

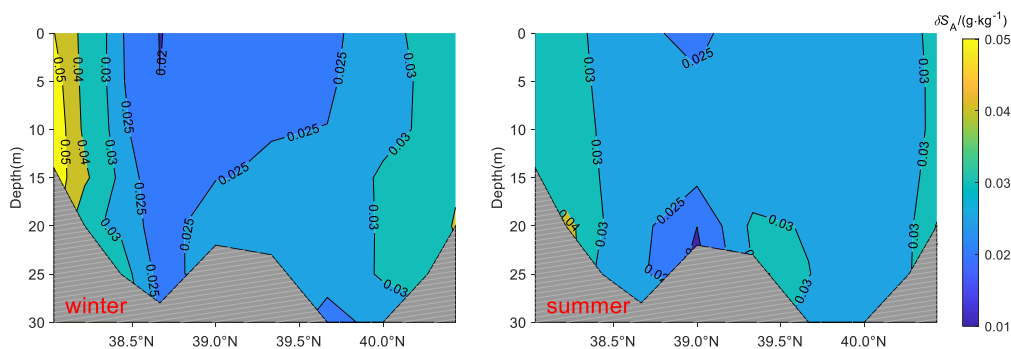
3.2 The Absolute Salinity Anomaly δS_A and Practical Salinity Anomaly δS_P of the Bohai Sea

As shown in Figs. 4, 5, and 6, the multi-year mean δS_A along Section B in the winter and summer based on Eq. (8) is the same as that of $\Delta[\text{HCO}_3^-]$, with the minimum value occurring in the middle, gradually increasing toward the southwest and northeast ends, the maximum value of $0.06 \text{ g} \cdot \text{kg}^{-1}$ is found at the estuary of the Yellow River in winter, and the remainder is greater than $0.01 \text{ g} \cdot \text{kg}^{-1}$, the δS_A is varying little along the vertical. Except for the two stations near the Yellow River estuary, the differences in δS_A between summer and winter were less than $0.01 \text{ g} \cdot \text{kg}^{-1}$ at the remaining eight sites.

Based on the MIEP data, the δS_A along Section B during the winter of 2007 was considerably higher than the multi-year average with the maximum $0.1 \text{ g} \cdot \text{kg}^{-1}$ found in the Bohai and Laizhou Bays.

180

The δS_P has the same spatial and temporal distribution as with δS_A the maximum 0.04 PSS-78 occurs in the Bohai and Laizhou Bays. Along Section B, excluding the two stations at the estuary of the Yellow River, the δS_P ranges from 0.01 to 0.02 PSS-78 , the δS_P of the other eight stations are basically around 0.01 PSS-78 , as shown in Figs. 6 and 7.



185

Figure 4. Multi-year mean δS_A isolines along Section B, the left is in winter and the right is in summer

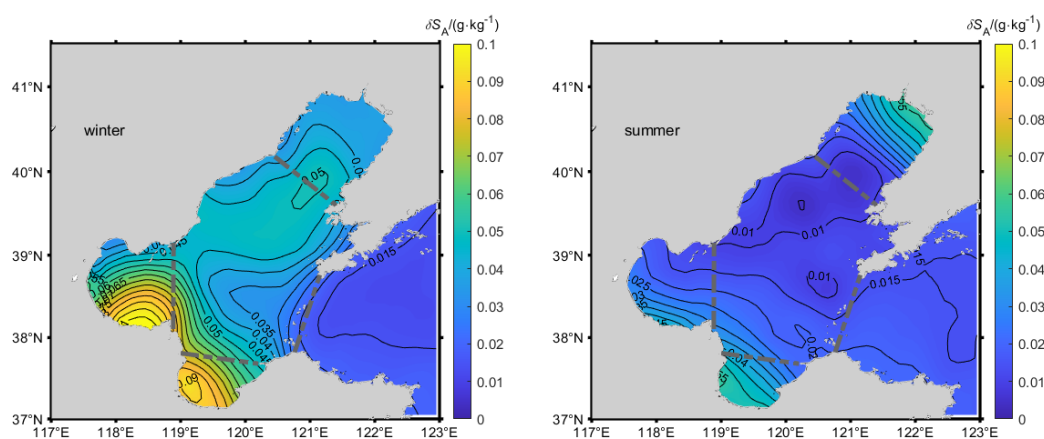
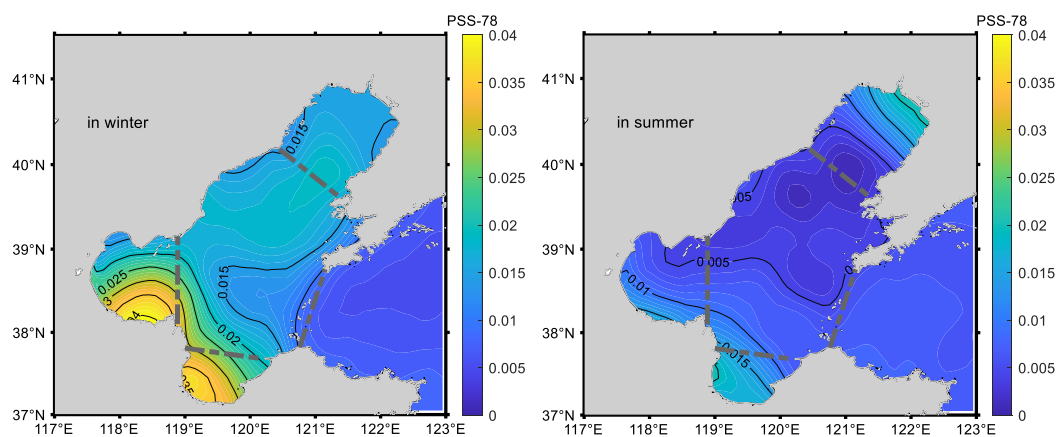


Figure 5. The δS_A isolines in the sea bottom of the Bohai Sea in the winter of 2007 and summer of 2006.



190 Figure 6. The δS_P isolines in the sea bottom of the Bohai Sea in winter of 2007 and summer of 2006.

Table 1. The multi-year mean δS_A and δS_P of the four stations of Section B

	B01	B04	B07	B10
--	-----	-----	-----	-----



$\delta S_{A_sum}/(g \cdot kg^{-1})$	0.035±0.010	0.026±0.008	0.029±0.007	0.032±0.01
$\delta S_{A_win}/(g \cdot kg^{-1})$	0.052±0.021	0.021±0.010	0.026±0.012	0.035±0.011
$\delta S_{P_sum}/(PSS-78)$	0.013±0.004	0.009±0.003	0.010±0.003	0.011±0.004
$\delta S_{P_win}/(PSS-78)$	0.025±0.008	0.009±0.004	0.010±0.005	0.016±0.005

It is found *that* δS_A has changed significantly in the Baltic Sea over the last 30 years (Feistel et al, 2009). It's necessary to study the patterns of change of δS_A and δS_P over the years based on the data of Section B which are found to characterize the spatial distribution of δS_A and δS_P in the Bohai Sea, excluding Laizhou and the Liaodong Bays. Based on the above result,

195 we picked four stations at equal intervals along Section B to investigate it.

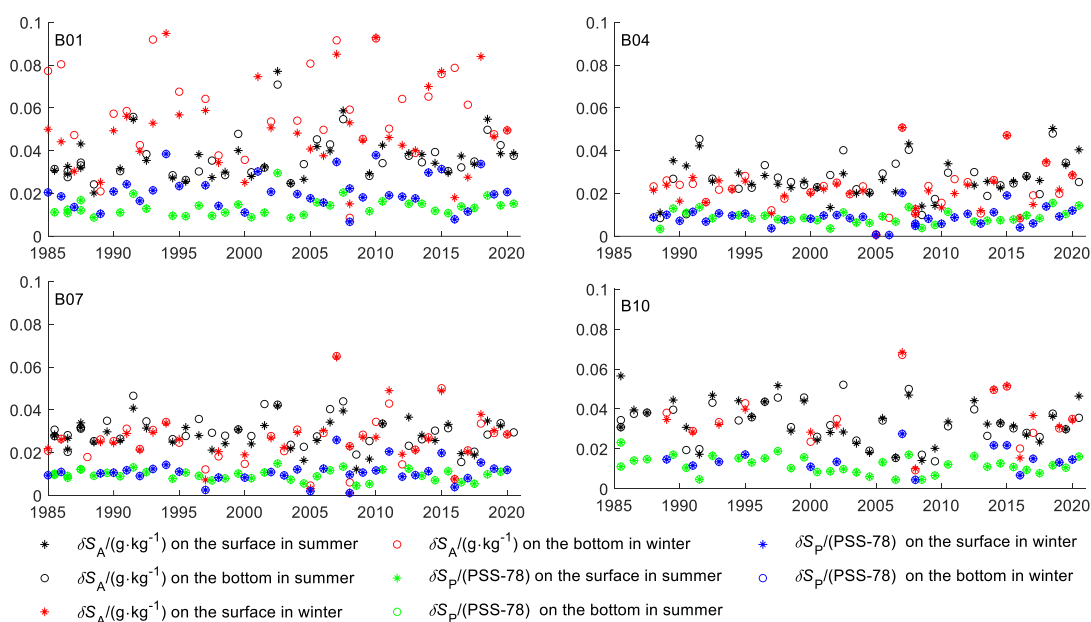


Figure 7: δS_A and δS_P of the stations B01, B04, B07 and B10 of Section B from 1985 to 2020

The δS_A of station B01, very near the Yellow River estuary, is not only significantly higher than the other stations, ranging from 0.02 to 0.1 $g \cdot kg^{-1}$ but also the seasonal variations and the differences between the bottom and the surface are more obvious than the other stations. δS_A is higher in winter than in summer and that on the bottom is greater than that on the surface. The correlation coefficients between δS_A of all four stations in summer and that in winter in the same year are around 0.1, indicating that the nutrients and inorganic carbon composition anomalies of station B01 will return to the common state in summer and not be carried over to the next year after the water exchange in and out of the Bohai Sea, geochemical processes, and biological consumption of that year, and there is no long-time change trend. Compared with station B01, δS_A is not only significantly reduced at the remaining three stations, B04, B07, and B10, but also the magnitude of the interannual variability is greatly attenuated, and the seasonal and vertical changes are less obvious.



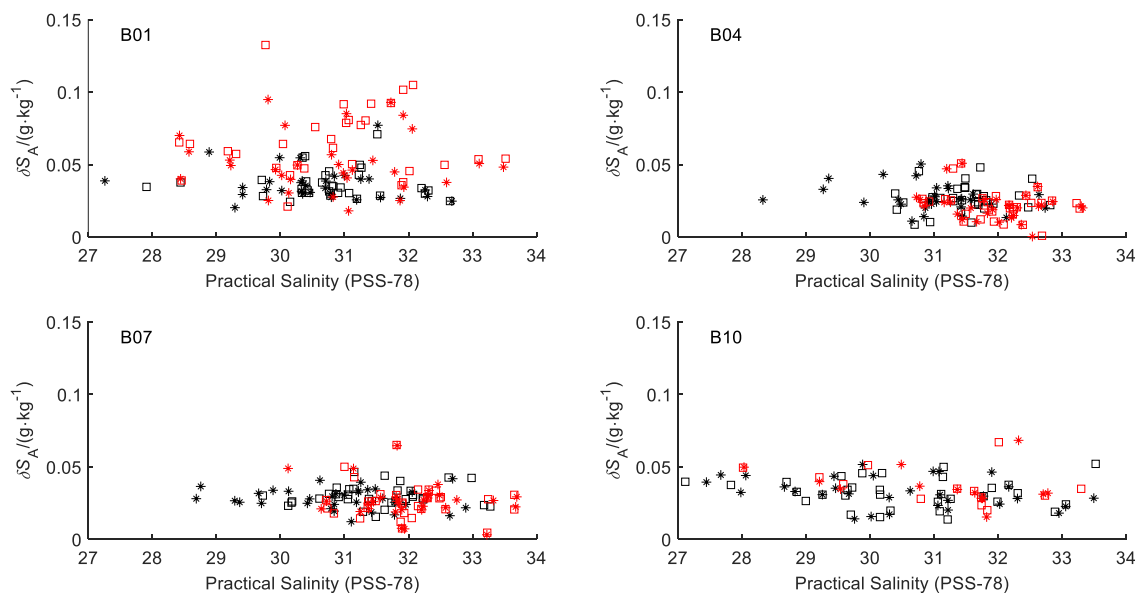
The temporal variations of δS_P along Section B are the same as that of δS_A , but only one-third to one-half of δS_A , with variations ranging from 0 to 0.04 PSS-78, implying that it is much more stable. This is because the small additional dissolved calcium carbonate in seawater affects the electrical conductivity much less than that of the same mass of NaCl which is the main solute of seawater.

3.3 Parameterization of δS_A and δS_P of the Bohai Sea

The Absolute Salinity of a seawater sample is usually calculated by treating the sample as a mixture composed of a known fraction f of SSW with $S_A = 35.16504$ and a fraction $1 - f$ of river water with a salinity of S_{RW} (Pawlowicz, 2015; Millero, 2013; Feistel et al, 2010), the equation is as follows,

$$S_A = S_R + \left(1 - \frac{S_R}{S_{SO}}\right) S_{RW} \quad (14)$$

Located in the East Asian monsoon region, the rainy season of the Bohai Sea is very short, and more than 70% of the annual Runoff of the Yellow River discharges into the Bohai Sea from July to November. Moreover, the result of annual total precipitation minus annual evaporation is usually much greater than that from 1985 to 2020 (Ji et al, 2023). So, the runoff of the Yellow River is neither a major source of freshwater nor a source of additional dissolved substances to the Bohai Sea. The relative composition anomalies $\Delta[\text{HCO}_3^-]$ and $\Delta[\text{Ca}^{2+}]$ originate mainly from suspended and re-solubilized sediments that are agitated and mixed by strong north winds in winter, largely independent of Practical Salinity which is controlled by freshwater budget as shown in Fig.8, so both the Eq. (6) provided by TEOS-10 and Eq. (14) can't apply to calculate the δS_A of the Bohai Sea.

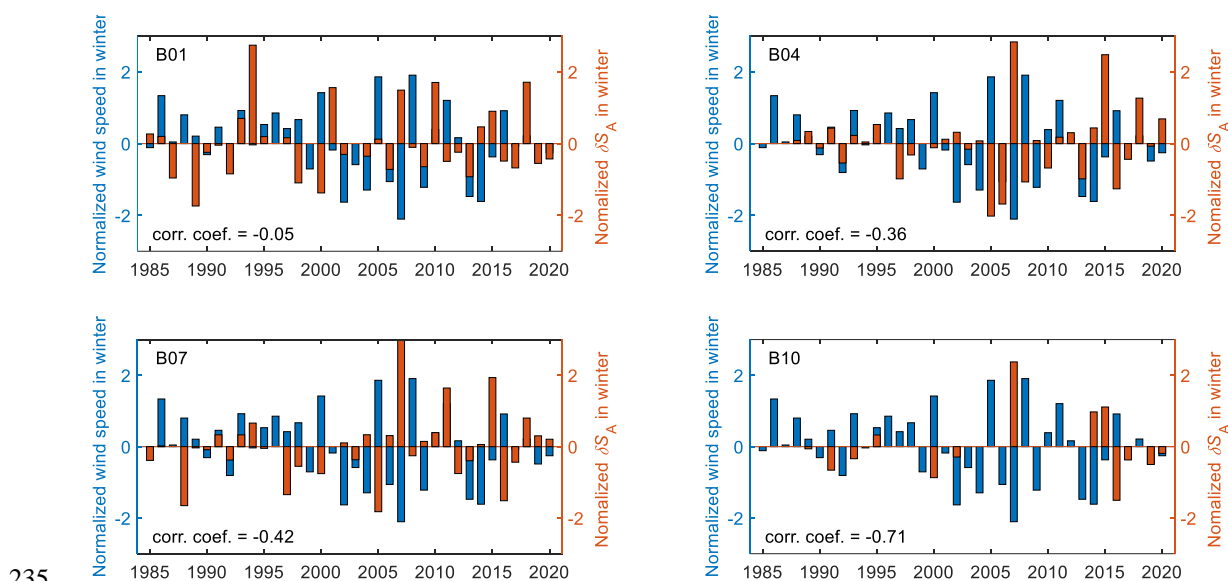


225

Figure 8: δS_A versus S_P of the 1st, 4th, 7th, and 10th stations of Section B from 1985 to 2020, symbols 'o' and '*' denote the surface and bottom data in winter, 'o' and '*' denote the surface and bottom data in summer.



230 Since the observation time of section B is limited to the winter and summer seasons, it is not possible to grasp the specific geochemical processes in the Bohai Sea, but the magnitude of δS_A changes in winter is significantly higher than that in summer and is independent of that in summer. According to previous research results, the average temperature of the Bohai Sea in winter is below 10°C and biological activities are not obvious, but the strong north wind that prevails in the Bohai Sea in winter is the main driving force for the exchange of water in and out of the Bohai Sea. Therefore, the correlation between the absolute salinity anomalies in winter and the average wind speed of the north wind at the four stations was analyzed, and the results are shown in Fig. 9.



235 **Figure 9: Normalized δS_A versus normalized averaged wind speed of the 1st, 4th, 7th, and 10th stations of Section B in winter from 1985 to 2020**

As shown in Fig. 9, the δS_A in winter, δS_{A_winter} , shows a moderately negative correlation with the mean wind speed along Section B in winter. However, the winter winds were weaker than usual in the year of the extreme values of δS_{A_winter} , so that winter water exchange had a greater influence on δS_{A_winter} than local geochemical processes.

240 According to the source and seasonal variation of relative composition anomalies, the equation for δS_A and δS_P in the Bohai Sea can be fitted based on the measurements of section B as follows,

$$\begin{aligned} \delta S_A &= \delta S_A(\Phi, \lambda, Summer/Winter) \\ \delta S_P &= \delta S_P(\Phi, \lambda, Summer/Winter) \end{aligned} \quad (15)$$

245 In which, Φ is the latitude, λ is the longitude. The δS_A and the δS_P of the four stations of Section B are listed in Table 1.

4 Discussion and conclusions



250 The local long-term trends in salinity are precisely measurable indicators for climatic changes in the terrestrial water cycle and its sensitivity to global warming (Durack et al 2013; Pawlowicz, 2016), but the salinity anomalies due to the relative composition anomaly of the semi-closed Bohai Sea have always been neglected in studies due to the lack of measurements and the possibility of changes in a relatively short period, which means that the level of uncertainty in salinity is even more unknown.

255 With the benefit of the repeat in-situ measurements along the section from 1985 to 2020 and the near-synchronous field data from 2006 to 2007 in the Bohai Sea, this study could accurately characterize the salinity anomalies arise from specific biogeochemical processes and specify the compatibility level of long-term salinity change with/without consideration of composition variations of the Bohai Sea.

The results of the study are outlined below: the relative chemical composition anomalies mainly originate from the suspension and re-dissolution of bottom sediments, with the higher proportion of dissolved inorganic carbon with significant seasonal and interannual variations resulting from the weak water exchange with the open ocean, give rise the Absolute Salinity up to $0.1 \text{ g}\cdot\text{kg}^{-1}$ through TEOS-10 methods, moreover, it increases the Practical Salinity of $0\sim 0.04 \text{ PSS-78}$.
260 With/without consideration of the relative composition variation, the uncertainty of S_A and S_P are $[0.01\sim 0.02]/[0.03\sim 0.06] \text{ g}\cdot\text{kg}^{-1}$ and $[0.0\sim 0.01]/[0.01\sim 0.03]$ respectively.

265 Since NaCl is the predominant solute in seawater, the effect of additional calcium carbonate dissolved in seawater on the conductivity is much smaller than that of the same mass of NaCl, and therefore locale relative component anomalies input to the Bohai Sea results in Absolute Salinity Anomalies that are twice to three times larger than the Practical Salinity Anomalies. If small variations in the relative dissolved composition of Bohai Sea water are ignored, the uncertainty in Practical Salinity is smaller than that in Absolute Salinity when analyzing salinity variations associated with climate.

270 Unlike the Baltic Sea, there is no obvious correlation between the relative composition anomalies in the Bohai Sea in winter and that in summer, so there is no cumulative effect of the relative composition anomalies and no apparent long-term trend from 1985 to 2020.

This work utilizes the results of ongoing research in cases where the exact chemistry compositions of the Bohai Seawater are not precisely known and ignores the effects of other unknown components due to the lack of measurements, such as the changes in sulfate, but all these procedures should not be applied in situations where the chemical composition may vary in other ways as a result of different processes. This will be improved in future work.

275 **Competing interests**

The contact author has declared that none of the authors has any competing interests.



References

- Chen, D.: Marine Atlas of Bohai Sea, Yellow Sea, East China Sea, Hydrology. China Ocean Press, Beijing. 530 pp. (in Chinese), 1992.
- 280 Commission of Science and Technology of the People's Republic of China: Report of the National Comprehensive Marine Survey, Volume I, 1964.
- Durack P., Wijffels S., and Boyer T.: Long-term salinity changes and implications for the global water cycle Ocean Circulation and Climate. A 21st Century Perspective ed G Siedler et al (Amsterdam: Elsevier) pp 727–57, 2013.
- Fan W., Xiang W., Wang H.: China Oceanographic Hydrometeorological and Climatological Records: Bohai Volume [M],
285 Beijing: Ocean Press, 2021.
- Feistel R., Weinreben S., Wolf H., Seitz S., Spitzer P., Adel B., Nausch G., Schneider B., and Wright D. G.: Density and Absolute Salinity of the Baltic Sea 2006–2009, Ocean Sci., 6, 3–24, <https://doi.org/10.5194/os-6-3-2010>, 2010b.
- Feistel R., Wielgosz R., Bell S., Camões M., Cooper J., Dexter P., Dickson A., Fisticaro P., Harvey A., Heinonen M., Hellmuth O., Kretzschmar H., Lovell J., McDougall T., Pawlowicz R., Ridout P., Seitz S., Spitzer P., Stoica D., and Wolf H.,
290 Metrological challenges for measurements of key climatological observables: oceanic salinity and pH, and atmospheric humidity. Part 1: Overview, Metrologia, 53, R1–R11, <http://iopscience.iop.org/0026-1394/53/1/R1>, 2016.
- GCOS: Implementation Plan for the Global Observing System for Climate in support of the UNFCCC (2010 Update) (Geneva: World Meteorological Organization) WMO-TD/No. 1532 (GCOS-138) p 180 www.wmo.int/pages/prog/gcos/Publications/gcos-138.pdf, 2010.
- 295 Guan B. and Chen S.: Report of the National Comprehensive Marine Survey, Volume I, 1964
- IOC, SCOR, IAPSO: The International Thermodynamic Equation of Seawater – 2010: Calculation and Use of Thermodynamic Properties. Manual and Guides No. 56, Intergovernmental Oceanographic Commission, UNESCO (English), 2010.
- Ji W.: China Offshore Oceans—Marine Chemistry [M], Beijing: Ocean Press, 2016.
- Ji F., Pawlowicz R., Xiong X.: Estimating the Absolute Salinity of Chinese offshore waters using nutrients and inorganic
300 carbon data, Ocean Sci., 17, 909–918, 2021 <https://doi.org/10.5194/os-17-909-2021>, 2021.
- Ji F., Xiong X.: Mechanisms of salinity anomalies in the Bohai Sea in winter 2007, submitted to Continental Shelf Research, 2023
- Lewis, E. and Wallace, D. W. R.: Program Developed for CO2 System Calculations, Github [Dataset], available at: <https://github.com/jamesorr/CO2SYS-MATLAB>, last access: 8 June 2021.
- 305 Lin C., Su J., Xu B.: Long-term variations of temperature and salinity of the Bohai Sea and their influence on its ecosystem, J. Progress in Oceanography, 49:7-19, 2001.
- Lv, C.: Analysis of decadal variability of salinity field and its influence to circulation in Bohai and northern Yellow Sea, The Master Degree Dissertation of China Ocean University, 2008.



- Ma C., Wu D., Lin X.: The interannual and long-term variation characteristics and causes of salinity in the Bohai Sea and the
310 Yellow Sea, *Journal of Ocean University of China, Natural Science Edition*, 36(Sup.), 7-12, 2006.
- McDougall, T. J. and Barker, P. M.: Getting started with TEOS-10 and the Gibbs Seawater (GSW) Oceanographic Toolbox,
28 pp., SCOR/IAPSO WG127, ISBN 978-0-646-55621-5, 2011.
- McDougall, T. J., Jackett, D. R., Millero, F. J., Pawlowicz, R., and Barker, P. M.: A global algorithm for estimating Absolute
Salinity, *Ocean Sci.*, 8, 1123–1134, <https://doi.org/10.5194/os-8-1123-2012>, 2012.
- 315 Millero, F. J., Feistel, R., Wright, D. G., and McDougall, T. J.: The composition of Standard Seawater and the definition of
the Reference-Composition Salinity Scale, *Deep-Sea Res. Pt. I*, 55, 50–72, 2008.
- Pawlowicz, R.: Calculating the conductivity of natural waters, *Limnol. Oceanogr.: Methods*, 6, 489–501, 2008.
- Pawlowicz, R.: A model for predicting changes in the electrical conductivity, practical salinity, and absolute salinity of
seawater due to variations in relative chemical composition, *Ocean Sci.*, 6, 361–378, <https://doi.org/10.5194/os-6-361-2010>,
320 2010.
- Pawlowicz, R.: The Absolute Salinity of seawater diluted by river water, *Deep-Sea Res. Pt. I*, 101, 71–79, 2015.
- Pawlowicz R., Feistel R., McDougall T. J., Ridout P., Seitz S., and Wolf, H.: Metrological challenges for measurements of
key climatological observables – Part 2: Oceanic salinity, *Metrologia*, 53, R12–R15, [https://doi.org/10.1088/0026-1394/53/1/
R12](https://doi.org/10.1088/0026-1394/53/1/R12), 2016.
- 325 Pawlowicz, R., Wright, D. G., and Millero, F. J.: The effects of biogeochemical processes on oceanic conductivity/salinity/
density relationships and the characterization of real seawater, *Ocean Sci.*, 7, 363–387, <https://doi.org/10.5194/os-7-363-2011>,
2011.
- Qi, D.: Dissolved calcium in the Yangtze River Estuary and China Offshore, The Master Degree Dissertation of Xiamen
University, 2013.
- 330 Seitz S., Feistel R., Wright D., Weinreben S., Spitzer P., and de Bievre P.: Metrological traceability of oceanographic salinity
measurement results *Ocean Sci.* 7 45–62, 2011, www.ocean-sci.net/7/45/2011/.
- UNESCO: The Practical Salinity Scale 1978 and the International Equation of State of Seawater 1980, UNESCO Technical
Papers in Marine Science, 36, 25 pp., 1981.
- Yu H., Bao X., Lü C., Chen X., Kuang L.: Analyses of the long-term salinity variability in the Bohai Sea and the northern
335 Huanghai(Yellow)Sea, *Acta Oceanologica Sinica*, Vol.28, No.5, p.1-8, 2009.
- Xiong X., *China Offshore Oceans—Physical Oceanography and Marine Meteorology [M]*, Beijing: Ocean Press, 2012
- Xu J.: The Variation Characters and Formation Mechanism of Salinity in the Bohai Sea, Ocean University of China, Master
Thesis (in Chinese), 2007.
- Zweng, M.M, J.R. Reagan, D. Seidov, T.P. Boyer, R.A. Locarnini, H.E. Garcia, A.V. Mishonov, O.K. Baranova, K.W.
340 Weathers, C.R. Paver, and I.V. Smolyar: World Ocean Atlas 2018, Volume 2: Salinity. A. Mishonov, Technical Editor, NOAA
Atlas NESDIS 82, 50pp. This document is available online at <http://www.nodc.noaa.gov/OC5/indprod.htm>, 2019.